RSC Advances

ROYAL SOCIETY OF CHEMISTRY

www.rsc.org/advances

Tailoring the Surface of Liquid Crystal Droplets with Chitosan/Surfactant complexes for the Selective Detection of Bile Acids in Biological Fluids

Tanmay Bera, Jinan Deng, and Jiyu Fang*

Department of Materials Science and Engineering, University of Central Florida
Orlando, FL 32816. USA. E-mail: Jiyu.Fang@ucf.edu. Tel: 1-407-882-1182

Abstract

We report an approach for tailoring the surface of 4-*n*-pentyl-4'-cyanobiphenyl (5CB) droplets by the adsorption of chitosan (CHI) at the 5CB/aqueous interface, followed by the penetration of sodium tetradecyl sulfate ($SC_{14}S$). The CHI/$SC_{14}S$ complex-coated 5CB droplets can be used as an optical probe for the detection of cholic acid (CA) in phosphate-buffered saline and urine without dilution. We find that the CHI coating can significantly reduce the detection limit of 5CB droplets for CA. By controlling the number of CHI/$SC_{14}S$ complex-coated 5CB droplets, the detection limit for CA can be changed from ~ 75 μM to ~ 0.5 μM, which covers the concentration range of CA in individual urine with and without intestinal diseases.

Keywords: Liquid crystal droplets, chitosan, surfactants, detection, and bile acids

1. Introduction

Liquid crystal (LC) droplets dispersed in aqueous solution are a stimuli-responsive soft material, in which the adsorption of chemical and biological species at the LC/aqueous interface may alter the surface anchoring energy, consequently changing the optical appearance of LC droplets.[1-2] Recently, there has been interest in tailoring the surface of LC droplets by the adsorption of polymers at the LC/aqueous interface for tuning the interaction of chemical and biological species with the LC droplets.[3] It has been shown that polyelectrolyte-coated LC droplets are permeable for surfactants. The surfactant penetrated through the polyelectrolyte coating is able to induce the radial configuration of the LC inside the droplet. A biosensor platform based on polyelectrolyte-coated LC droplets was developed for detecting lipid-enveloped viruses, in which the transfer of lipids from the viruses into the polyelectrolyte-coated LC droplets induced the bipolar-to-radial configuration transition of the LC droplets.[3b] The radial-to-bipolar transition of polyelectrolyte-coated LC droplets, which is a result of the disruption of the surfactant penetrated in the polyelectrolyte-coated LC droplets due to the formation of anti-IgG/IgG complexes on the surface of the LC droplets, was used as a sensor platform for the development of immunoassays.[3d]

Chitosan (CHI) is a natural polyelectrolyte (Figure 1a). The interaction of CHI with bile acids and lipids plays an important role for reducing cholesterol in the small intestine.[4] Here, we tailor the surface of 4-*n*-pentyl-4'-cyanobiphenyl (5CB) droplets dispersed in aqueous solution by the adsorption of CHI at the 5CB/aqueous interface, followed by the penetration of sodium tetradecyl sulfate ($SC_{14}S$). CHI/$SC_{14}S$ complex-coated 5CB droplets are used as an optical probe for the selective detection of cholic acid (CA) (Figure 1b) in biological fluids with uric acid, ascorbic acid, and urea by simply observing their configuration transitions with the naked eye under a polarizing optical microscope. We find

that the CHI coating can reduce the detection limit of the 5CB droplets for CA. The detection limit of CHI/$SC_{14}S$ complex-coated 5CB droplets for CA can be altered over a range from ~ 75 μM to ~ 0.5 μM by controlling the number of the droplets.

2. Results and Discussion

Figure 2a shows a polarizing optical microscopy image of CHI-coated 5CB droplets formed in aqueous solution at pH 4.5. The positively charged CHI-coated 5CB droplets show a bipolar configuration, suggesting a parallel surface anchoring of the 5CB inside the droplets. The diameter of CHI-coated 5CB droplets is 0.76 ± 0.21 μm. The ζ-potential of CHI-coated 5CB droplets is + 38 mV. After the addition of 9 μM negatively charged $SC_{14}S$, the ζ-potential of CHI-coated 5CB droplets reduces to + 22 mV due to the adsorption of $SC_{14}S$ in the CHI-coated 5CB droplets. The CHI/$SC_{14}S$ complex-coated 5CB droplets have a radial configuration (Figure 2b), suggesting a perpendicular anchoring of the 5CB in the droplets. It has been shown that the adsorption of $SC_{14}S$ at the 5CB/aqueous interface of 5CB droplets dispersed in aqueous solution can induce a radial configuration of the 5CB inside the droplets.[5] Therefore, we conclude that $SC_{14}S$ is able to penetrates into the CHI coated-5CB droplets, in which the negatively charged head group of the $SC_{14}S$ is located in the positively charged CHI coating due to electrostatic attraction and the hydrophobic tail of the $SC_{14}S$ penetrates into the 5CB droplets to induce the radial configuration. To verify the stability of the CHI coating after the adsorption of $SC_{14}S$, we tailored the surface of 5CB droplets dispersed in aqueous solution at pH 4.5 by the adsorption of FITC-labeled CHI at the 5CB/aqueous interface. FITC-labeled CHI was synthesized according to the method reported in the literature.[6] The details of the synthesis of FITC-labeled CHI was given in experimental section. Under a bright field microscope, FITC-labeled CHI-coated 5CB droplets show two defect points at the opposite poles of the droplets (Figure 2c), representing the bipolar

configuration.[1] When being excited with 488 nm light, the FITC-labeled CHI-coated 5CB droplets show green emission (Figure 2d). After the adsorption of $SC_{14}S$, the FITC-labeled CHI-coated 5CB droplets show a single defect at the center of the droplets (Figure 2e), representing the radial configuration.[1] The green emission from the radial droplets is still visible (Figure 2f), which suggests that the CHT coating remains stable after the adsorption and penetration of $SC_{14}S$.

The SC_nS penetration-induced bipolar-to-radial transition of CHI-coated 5CB droplets is also observed for n = 12, 16, and 18. For the same amount of CHI-coated 5CB droplets (~ 8.5×10^8 mL^{-1}), the minimum concentration of SC_nS required to inducing the bipolar-to-radial transition of CHI-coated 5CB droplets is ~ 28 μM $SC_{12}S$, ~ 9 μM for $SC_{14}S$, ~ 7 μM for $SC_{16}S$, and ~ 3 μM for $SC_{18}S$, respectively (Figure 3). These concentrations are significantly lower than that of SC_nS required to inducing the radial configuration of naked 5CB droplets dispersed in aqueous solution (~ 5 mM),[5a] which suggests that the CHI-coating lows the surface density of SC_nS molecules required to induce a radial configuration of 5CB droplets. Past studies showed that the surface anchoring energy increases with the increase of the hydrophobic tail length of the surfactant adsorbed at the surface of liquid crystals.[7] The hydrocarbon tail length of the SC_nS protruded from the CHI coating into the 5CB droplets increases with n. This may explain why the concentration of SC_nS required to inducing the bipolar-to-radial transition of CHI-coated 5CB droplets decreases with the increase of n (Figure 3). There is no radial CHI/SC_nS complex-coated 5CB droplet observed for n < 12.

Bile acids are a biomarker for the diagnosis of liver and intestinal diseases.[8] For healthy individuals, the level of bile acids in urine is less than 7 μM,[9] which increase to 10 - 100 μM for individuals with liver and intestinal diseases.[10] Thus, the analysis of bile acids in urine is often used for diagnosing liver disease and evaluating the effectiveness of

treatments.[11] Our previous studies showed that SC_nS-coated 5CB droplets could be used as an optical probe for the detection of bile acids, in which the disruption/removal of the SC_nS from the surface of the 5CB droplets by the competitive adsorption of bile acids induced the radial-to-bipolar transition of the 5CB droplets.[5a] Thus, a possible method for lowing the detection limit of the 5CB droplets is to low the packing density of the SC_nS at their surfaces. Here, we exploit the application of CHI/SC_nS complex-coated 5CB droplets with the radial configuration formed by using SC_nS with minimum concentrations (Figure 3) for the detection of CA. Figures 4a-4b show the polarizing optical microscopy images of CHI/$SC_{14}S$ complex-coated 5CB droplets in PBS solution at pH 7.5 before and after the CA. In our experiments, CHI/$SC_{14}S$ complex-coated 5CB droplets formed in aqueous solution at pH 4.5 were purified through centrifugation and then re-dispersed in PBS solution. The radial CHI/$SC_{14}S$ complex-coated 5CB droplets remain stable in PBS solution and show the ζ-potential of + 7 mV. After the addition of CA, we find that CHI/$SC_{14}S$ complex-coated 5CB droplets transit from the radial configuration to the bipolar configuration. The adsorption of CA is evident from the ζ-potential change of CHI/$SC_{14}S$ complex-coated 5CB droplets from + 7 mV to – 5mV.

CA is a facial amphipathic molecule with a hydrophobic concave α face and a hydrophilic convex β face (Figure 1b).[8] It has been shown that amphipathic CA can remove lipids from the oil-water interface through emulsification, in which the hydrophobic tail of the removed lipid is buried in the hydrophobic environment of CA micelles.[12] The disruption/removal of lipids from the surface of the 5CB droplets dispersed in aqueous solution by the competitive adsorption of amphipathic CA is also reported in the literature.[5a] For the CHI/$SC_{14}S$ complex-coated 5CB droplets, the adsorption of amphipathic CA disrupts the packing of the $SC_{14}S$ at the surface of the 5CB droplets. The director configuration of CHI/$SC_{14}S$ complex-coated 5CB droplets is determined by the balance between the elasticity

and the surface anchoring energy of the 5CB inside the droplets. Past studies showed that the surface anchoring energy depended on the packing of the surfactant at the surface of liquid crystals.[13] The disruption of the packing of the $SC_{14}S$ at the surface of the 5CB droplets by the adsorption of the amphipathic CA may change the surface anchoring energy, consequently inducing the radial-to-bipolar transition. A schematic illustration of the CA-induced configuration transition of CHI/$SC_{14}S$ complex-coated 5CB droplets is shown in Figures 4c-4d.

The radial-to-bipolar transition of CHI/$SC_{14}S$ complex-coated 5CB droplets is found to depend on the concentration of CA in PBS solution. For the comparison, we plot the transition curves of CHI/$SC_{14}S$ complex-coated 5CB droplets and $SC_{14}S$-coated 5CB droplets as a function of CA concentrations together (Figure 4e), in which the total number of the droplets is kept the same (~ 8.5×10^8 mL^{-1}). For CHI/$SC_{14}S$ complex-coated 5CB droplets, the radial-to-bipolar configuration transition starts at the CA concentration of ~ 75 μM, which is defined as the detection limit. The transition curve of $SC_{14}S$-coated 5CB droplets shifts to the right, compared to that of CHI/$SC_{14}S$ complex-coated 5CB droplets. As can be seen in Figure 4f, the detection limit of CHI/$SC_{14}S$ complex-coated 5CB droplets for CA is lower than that of $SC_{14}S$-coated 5CB droplets (~ 150 μM). This is because the CHI coating lows the packing density of the $SC_{14}S$ molecules at the surface of the 5CB droplets, consequently reducing the surface anchoring energy of the radial-to-bipolar transition. The loosely packed SCS at the surface of the 5CB droplets is more easily disrupted by CA, which may explain the reduced detection limit of CHI/$SC_{14}S$ complex-coated 5CB droplets for CA.

The transition curves of CHI/SC_nS complex-coated 5CB droplets as a function of CA concentrations in PBS solution gradually shift to the left with the decrease of n (Figure 5a), in which the total number of the droplets was kept the same (~ 8.5×10^8 mL^{-1}). The detection

limit of CHI/SC_nS complex-coated 5CB droplets for CA goes down from ~ 240 μM to ~ 40 μM when n decreases from 18 to 12 (Figure 5b). The tail length of the SC_nS protruded from the CHI coating into the 5CB droplets is expected to decreases with the decrease of n. Thus, the SC_nS with shorter tails at the surface of the 5CB droplets is more easily disrupted by CA, which explains the decrease of the detection limit of CHI/SC_nS complex-coated 5CB droplets with the decrease of n. Although CHI/$SC_{12}S$ complex-coated 5CB droplets have the lowest detection limit for CA, they are not very stable over time due to the weak interaction of the penetrated $SC_{12}S$ with the 5CB droplets. Thus, we focused on the CA detection by using CHI/$SC_{14}S$ complex-coated 5CB droplets as an optical probe. We find that the transition curves of CHI/$SC_{14}S$ complex droplets gradually shift to the left by decreasing the number of the droplets (Figure 6a). The detection limit of CHI/$SC_{14}S$ complex-coated 5CB droplets for CA in PBS solution near linearly drops from ~ 75 μM to ~ 0.5 μM when the number of the droplets is reduced from ~ 8.5×10^8 mL^{-1} to ~ 1.5×10^6 mL^{-1} (Figure 6b).

The radial-to-bipolar transition of CHI/$SC_{14}S$ complex-coated 5CB droplets is also observed after the addition of deoxycholic acid (DCA), chenodeoxycholic acid (CDCA), and lithocholic acid (LCA) (Figure 7a), in which the total number of the droplets was kept the same (~ 8.5×10^8 mL^{-1}). CA bears three hydroxyl groups, DCA and CDCA bear two hydroxyl groups, while LCA only bears one hydroxyl group. The hydrophobicity of these bile acids is in the order: LCA > DCA > CDCA > CA.[14] It can be seen in Figure 7b, the detection limit of CHI/$SC_{14}S$ complex-coated 5CB droplets for these bile acids in PBS solution decreases with the increase of their hydrophobicity because more hydrophobic bile acids are more effective in the disruption of the packing of the $SC_{14}S$ at the surface of the 5CB droplets.

CA is a primary bile acid which comprises 31% of the total bile acids produced in liver. The correlation of liver and intestinal diseases with CA is much stronger than that of

other bile acids.[15] Therefore, we focused on the detection of CA in urine with CHI/$SC_{14}S$ complex-coated 5CB droplets. Ascorbic acid (AA), uric acid (UA), and urea are potential interference species for the detection of CA in urine.[16] However, we find that there is no radial-to-bipolar configuration transition for the CHI/$SC_{14}S$ complex-coated 5CB droplets in PBS solution even after the addition of 500 μM AA and 500μM UA, respectively (Figure 8). The selectivity of CHI/$SC_{14}S$ complex-coated 5CB droplets for CA over AA and UA, and urea may associate with their amphiphilic nature. The radial-to-bipolar transition of CHI/$SC_{14}S$ complex-coated 5CB droplets induced the competitive adsorption of amphiphilic CA at the surface of the droplets, which disrupts the packing of the $SC_{14}S$. While AA and UA are unable to adsorb at the surface of the 5CB droplets to disrupt the packing of the $SC_{14}S$ due to lacking the amphiphilic nature. Furthermore, we performed the detection of CA in PBS solution with 250 μM AA and 250 μM UA with CHI/$SC_{14}S$ complex-coated 5CB droplets. The transition curves of the 5CB droplets as a function of CA concentrations are near the same with and without AA and UA (Figure 9), in which the total number of the droplets is kept the same (1.5×10^6 mL^{-1}). Synthetic urine contains 280-350 mM urea and bovine urine has 149-166 mM urea and 8.9-29.7 mM UA. We find that there is no significantly change for the transition curves in synthetic urine and bovine urine, compared to PBS solution (Figure 9), suggesting that the presence of AA, UA and urea does not interfere the detection of CHI/$SC_{14}S$ complex-coated 5CB droplets for CA. The detection limit of CHI/$SC_{14}S$ complex-coated 5CB droplets for CA in synthetic urine and bovine urine is ~ 0.5 μM. A further reduction of the number of the droplets is expected to give even lower detection limit, but makes the detection difficult because there are only a few of droplets appeared in the microscopy field of the detection solution. Chromatography mass spectrometry is a common method for the detection of bile acids.[17] Although the precision and selectivity of the method is high, it is time consuming and requires expensive instruments. For the clinical diagnosis of liver and intestinal diseases, it is highly desirable to develop simple and rapid sensors for the

detection of bile acids in urine. Recently, electrochemical sensors based on enzyme reactions have been developed for the detection of CA in diluted urine with the detection limit of ~ 2 μM,[18] which is higher than that of CHI/$SC_{14}S$ complex-coated 5CB droplets. Compared to the electrochemical sensors, the 5CB droplet-based optical sensors are simple and rapid without needing complex detection systems and urine dilutions.

In conclusion, we report an approach to tailor the surface of 5CB droplets dispersed in aqueous solution by CHI/$SC_{14}S$ complexes. The CHI/$SC_{14}S$ complex-coated 5CB droplets can be used as an optical probe to detect CA in biological fluids without dilution. We find that the CHI coating is able to reduce the detection limit of the 5CB droplets for CA. By varying the number of CHI/$SC_{14}S$ complex-coated 5CB droplets, the detection limit for CA can be linearly changed from 75 μM to 0.5 μM, which covers the physiological concentration range of CA in individual urine with and without intestinal diseases. Our results highlight the possibility of using polyelectrolyte coatings to tune the interaction of bile acids and surfactants at the surface of 5CB droplets towards designing 5CB droplet based sensors for the sensitive and selective detection of bile acids in biological fluids.

4. Experimental Section

Materials: 4-cyano-4'-pentylbiphenyl (5CB, 98% purity), cholic acid (CA, ≥ 98% purity), deoxycholic acid (DCA, ≥ 98% purity), chenodeoxycholic acid (CDCA, ≥ 98% purity), lithocholic acid (LCA, ≥ 98% purity), sodium alkyl sulfate (SC_nS, n = 12, 14, 16, and 18, 99% purity), uric acid (UA, 98% purity), ascorbic acid (AA, 98% purity), urea, and chitosan (CHI, M_w ~ 190 kDa) were purchased from Sigma-Aldrich. Fluorescein isothiocyanate was obtained from Alfa Aesar. Phosphate-buffered saline was from Sigma-Aldrich. Synthetic urine was purchased from RICCA Chemical Company (Arlington, TX). Bovine urine was collected from a local slaughter house. All chemicals were used without further purification. Water

used in our experiments was purified using an Easypure II system (18.2 MΩ cm and pH 5.7). FITC-labeled CHI was synthesized based on the reaction between the isothiocyanate group of FITC and the primary amino group of CHI. Briefly, 0.1wt % CHI solution was prepared by dissolving CHI in 1% acetic acid solution. 1mg/mL of FTIC dissolved in ethanol was then added into 1 mL of the CHI solution. After 24 hours of the reaction in dark at room temperature, FITC-labeled CHI was precipitated by raising the pH to 9.0. Finally, the precipitated FITC-labeled CHI was centrifuged and washed repeatedly with water.

Preparation of CHI/SC$_n$S complex-coated 5CB droplets: CHI-coated 5CB droplets were formed by adding 10 μL 5CB in 10 mL of 0.1 wt% CHT aqueous solution at pH 4.5. The mixed solution was sonicated in a bath sonicator for 15 min. The resultant CHI-coated 5CB droplets were then washed twice through centrifugation to remove excess CHI and re-dispersed in aqueous solution at pH 4.5. SC$_n$S with desired concentrations was then added to CHI-coated 5CB droplet solution for 30 min. The concentration of CHI/SC$_n$S complex-coated 5CB droplets in aqueous solution was estimated with an optical microscope (Olympus BX40), in which a drop (2 μL) of CHI/SC$_n$S complex-coated 5CB droplet solution was placed between two cover glass slides and a large number of optical microscopy images were captured to represent the whole sample area. The number of the droplets confined by the two cover glass slides was carefully counted from the optical microscopy images and then used to calculate their concentrations in the initial solution. The final concentration of CHI/SC$_n$S complex-coated 5CB droplets used for the detection of CA was adjusted.

Characterization: The director configuration of CHI/SC$_n$S complex-coated 5CB droplets in aqueous solution was analyzed with a polarizing optical microscope (Olympus BX40) in transmission mode. ζ-potential measurements were carried out using Zetasizer Nano ZS90 (Malvern Instruments Inc.) at room temperature under a cell-driven voltage of 30 V. Confocal

fluorescence images were acquired with a Zeiss Axioscope-2 MOT microscope with 488 nm excitation from an Ar^+ laser.

Detection of bile acids with CHI/SC_nS complex-coated 5CB droplets: Bile acids were added into PBS, synthetic urine and bovine urine solution containing CHI/SC_nS complex-coated 5CB droplets. The mixed solution was incubated for 30 min. A drop (2 μL) of the mixed solution was placed between two cover glass slides. A large number of polarizing optical microscopy images of CHI/SC_nS complex-coated 5CB droplets was captured and then analyzed to estimate the percentage of the droplets, which underwent the director configuration transition. The data points shown in Figures 2-4 were obtained from the statistical result of 100 droplets from each sample.

Acknowledgements

This work was supported by US National Science Foundation (CBET-1264355).

References:

1. G. E. Volovik, O. D. Lavrentovich, *Sov. Phys. JETP.* 1983, **58**, 1159-1167.
2. D. S. Miller, X. Wang, N. A. Abbott, *Chem. Mater.* 2014, **26**, 496-506.
3. a) E, Tjipto, K. D. Cadwell, J. F. Quinn, A. P. R. Johnston, F. Caruso, N. L. Abbott, *Nano Lett.* 2006, **6***,* 2243-2248.; b) S. Sivakumar, K. L. Wark, J. K. Gupta, N. L. Abbott, F. Caruso, *Adv. Funct. Mater.* 2009, **19**, 2260–2265.; c) J. Zou, T. Bera, A. A. Davis, W. Liang, J. Y. Fang, *J. Phys. Chem. B.* 2011, **115**, 8970-8974.; d) V. A. Aliño, J. Pang, K. L. Yang, *Langmuir* 2011, **27**, 11784-11789.; e) W. Khan, J. H. Choi, G. Kim, S. Y. Park, *Lab on a Chip*. 2011, **11**, 3493-3498.; f) T. Bera, J. Y. Fang, *J. Mater. Chem.* 2012, **22**, 6807-6812.; g) U. Manna, Y. Zayas-Gonzalez, R. J. Carlton, F. Caruso, N. L. Abbott, D. M. Lynn, *Angew. Chem. Int. Ed.* 2013, **52**, 14011-14015.; h) J. Kim, M. Khan, S. Y. Park, *ACS Appl. Mater. Interfaces* 2013, **5**, 13135-13139.; i) T. Bera, J. Y. Fang, *J. Phys. Chem. B* 2014, **118**, 4970-4977.; j) S. H. Yoon, K. C. Gupta, J. S. Borah, S. Y. Park, Y. K. Kim, J. H. Lee, I. K. Kang, *Langmuir* 2014, **30**, 10668-1077.; k) J. Deng, X. Lu, C. Constant, A. Dogariu, J. Y. Fang, *Chem. Commun.* 2015. **51**, 8912-8915.
4. a) K. Y. Ebihara, B. O. Schneeman, *J. Nutr.*1989, **119**, 1100-1106.; b) K. M. Shields, N. Smock, C. E. McQueen, P. J. Bryant, *Am. J. Health Syst. Pharm.* 2003, **60**, 1310-1312.
5. a) T. Bera, J. Y. Fang, *Langmuir* 2013*,* **29**, 387-392.; b) T. Bera, J. Y. Fang, *J. Mater. Sci. Chem. Eng.* 2014, **2**, 1-7.
6. P. Tallury, S. Kar, S. Bamrungsap, Y. F. Huang, W. Tand, S. Santra, *Chem. Commun.* 2009, 2347-2349.
7. S. M. Malone, D. K. Schwartz, *Langmuir* 2008, **24**, 9790-9794.
8. A. F. Hofmann, R. Hagey, *Cell. Mol. Life Sci.* 2008, **65**, 2461-2483.
9. a) K. Rani, P. Garg, C. S. Pundir, *Anal. Biochem*. 2004, **332**, 32-37.; b) B. Alme, A. Bremmelgaard, J. Sjovall, P. Thomassen, *J. Lipid Res.*1977, **18**, 339-362.; c) I. Makino, M. Hashimoto, K. Shinozaki, K. Yoshino, S. Nakagawa, *Gastroenterology* 1975, **68**, 545-553.

10. A. Stiehl, Bile salt sulphates in cholestasis. *Eur. J. Clin. Invest*. 1974, **4**, 59-63.

11. a) S. Fischer, U. Beuers, U. Spengler, F. M. Zwiebel, H. G. Koebe, *Clinica Chimica Acta* 1996, **251**, 173-186.; b) F. Jorquera, M. J. Monte, J. Guerra, S. Sanchez-Campos, J. A. Merayo, J. L. Olcaz, J. Gonzalez-Gallego, J. G. Marin, *J. Gastroenterol. Hepatol.* 2005, **20**, 547-554.; c) S. P. R. Bathena, R. Thakare, N. Gautam, S. Mukherjee, M. Olivera, J. Meza, A. Alnouti. *Toxicol. Sci.* 2015, **143**, 296-307.

12. D. J. Cabral, J. A. Hamilton, D. M. Small, *J. Lipid Res.* 1986, **27**, 334-343.

13. a) J. Y. Fang, U. Gehlert, R. Shashidhar, C. M. Knobler, *Langmuir* 1999, **15**, 297-299.; b) J. M. Brake, N. L. Abbott, *Langmuir* 2002, **18**, 6101-6109.; c) A. D. Price, D. K. Schwartz, *J. Phys. Chem. B* 2007,**111**, 1007-1015.

14. M. J. Armstrong, M. Carey, *J .Lipid Res.* 1982, **23**, 70-80.

15. W. J. Griffiths, J. Sjövall, *J. Lipid Res.* 2010, **51**, 23-41.

16. a) F. Martinello, E. L. da Silva. *Clin. Biochem*. 2006, **39**, 396-403.; b) M. L. Brigden, D. Edgell, M. McPherson, A. Leadbeater, G. Hoag, *Clin. Chem.* 1991, **38**, 426-431.; c) M. Zwelg, A. Jackson, *Cline. Chem.* 1986, **32**, 674-677.

17. a) A. H. Que, T. Konse, A. G. Baker, M. V. Novotny, *Anal. Chem*. 2000, **72**, 2703-2710.; b) S. Perwaiz, B. Tuchweber, D. Mignault, T. Gilat, I. M. Yousef, *J. Lipid Res*. 2001, **42**, 114- 119.

18. a) S. Koide, N. Ito, I. Karube, *Biosens. Bioelectron*. 2007, **22**, 2079-2085.; b) B. Bartling, L. Li, C. Liu, *Analyst* 2009, **134**, 973-979.

Figure Captions

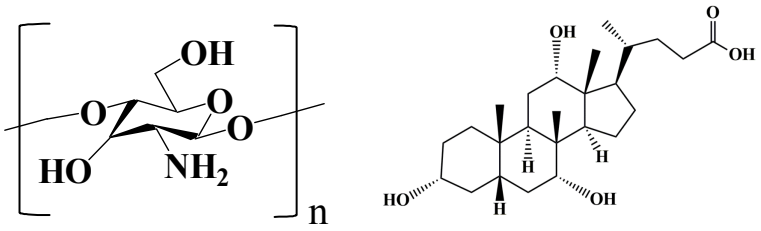

CHI CA

Figure 1. Chemical structure of CHI and CA

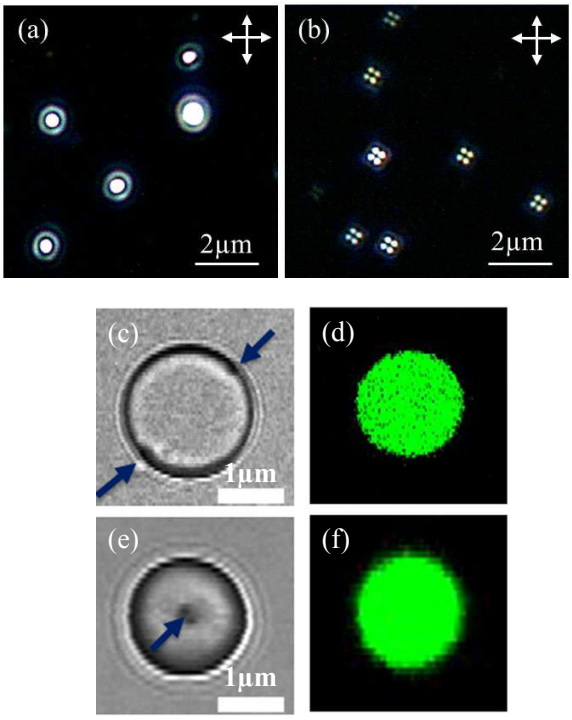

Figure 2. Polarizing optical microscopy images of CHI-coated 5CB droplets in aqueous solution at pH 4.5 before (a) and after (b) addition of 9 μM $SC_{14}S$. (c) and (e) Bright-field microscopy and (d) and (f) confocal fluorescence images of FITC-labeled CHI-coated 5CB droplets before and afte the addition of 9 μM $SC_{14}S$. The direction of the polarizer and analyzer is indicated by white arrows in (a) and (b). The arrows shown in (c) and (e) indicate the defects of bipolar and radial 5CB droplets.

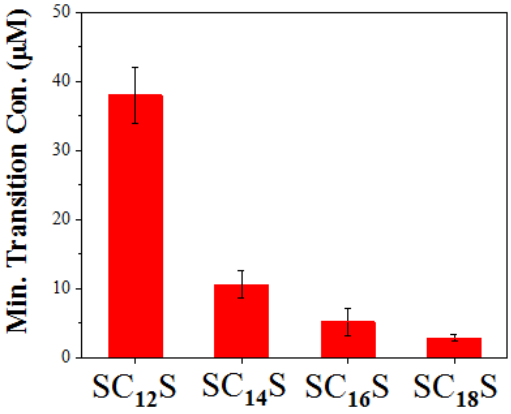

Figure 3. Miminum cconcentrations of SC_nS required to inducing the bipolar-to-radial transition of CHI-coated 5CB droplets in aqueous solution at pH 4.5.

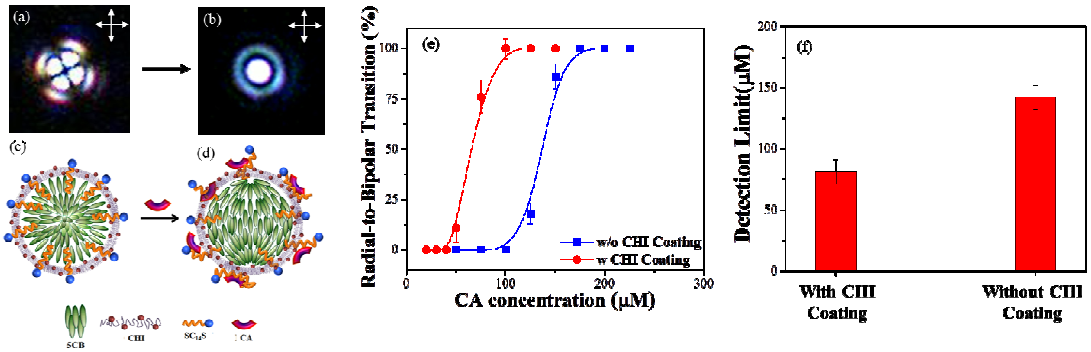

Figure 4. Polarizing optical microscopy images of CHI/$SC_{14}S$ complex-coated 5CB droplets in PBS solution at pH 7.4 before (a) and after (b) addition of 100 μM CA. Schematic illustration of the radial (c) and bipolar (d) configuration of the 5CB droplets. (e) The bipolar-to-radial transition curves of CHI/$SC_{14}S$ complex-coated 5CB droplets and $SC_{14}S$-coated 5CB droplets as a function of CA concentrations. (f) The detection limit of CHI/$SC_{14}S$ complex-coated 5CB droplets and $SC_{14}S$-coated 5CB droplets for CA in PBS solution. The direction of the polarizer and analyzer is indicated by white arrows in (a) and (b).

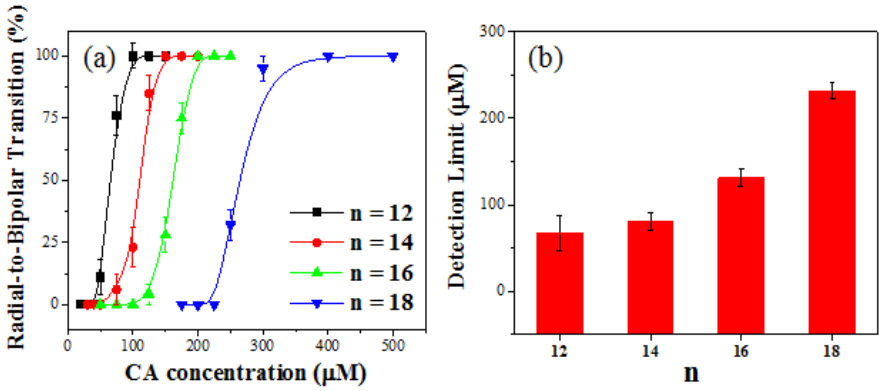

Figure 5. (a) The bipolar-to-radial transition percentage of CHI/SC_nS complex-coated 5CB droplets as a function of CA concentrations. (b) The detection limit of CHI/SC_nS complex-coated 5CB droplets for CA as a function of n. The number of the droplets was ~ 8.5 $\times 10^8$ mL^{-1}. The data points shown in (a) were obtained from the statistical result of 100 droplets from each sample.

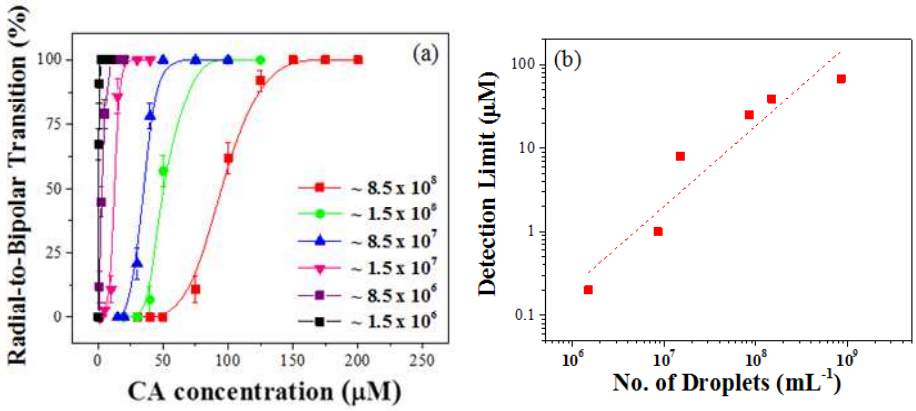

Figure 6. (a) The bipolar-to-radial transition curves of CHI/$SC_{14}S$ complex-coated 5CB droplets as a function of CA concentrations and a number of the droplets. (b) The detection limit of CHI/$SC_{14}S$ complex-coated 5CB droplets as a function of a number of the droplets. The data points shown in (a) were obtained from the statistical result of 100 droplets from each sample

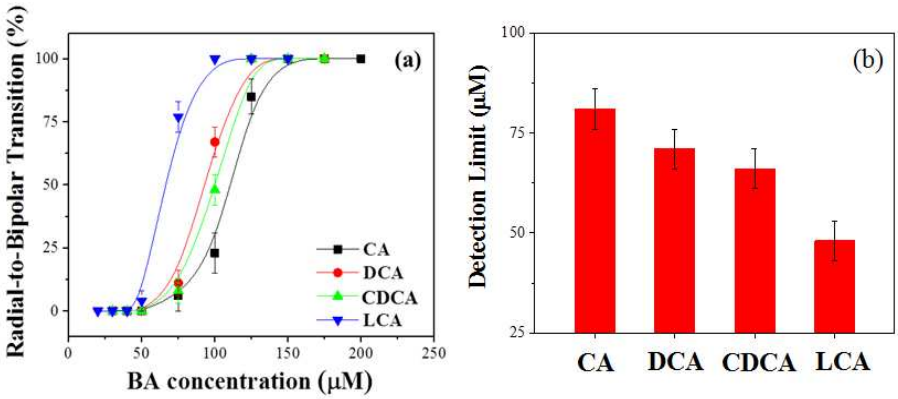

Figure 7. (a) The bipolar-to-radial transition percentage of CHI/$SC_{14}S$ complex-coated 5CB droplets as a function of the concentration of bile acids (BA). (b) The detection limit of CHI/$SC_{14}S$ complex-coated 5CB droplets for CA, DCA, CDCA, and LCA. The number of the droplets was ~ 8.5 $\times 10^8$ mL^{-1}. The data points shown in (6) were obtained from the statistical result of 100 droplets from each sample.

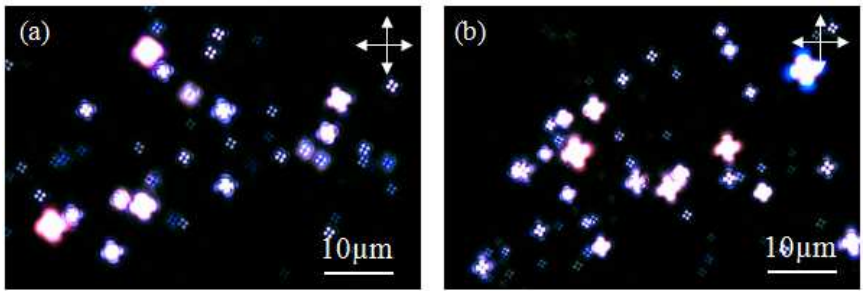

Figure 8. Polarizing optical microscopy images of CHI/$SC_{14}S$ complex-coated 5CB droplets in aqueous solution after the addition of 500 μM urea (a) and 500 μM uric acid (b). The number of the droplets was ~ 8.5 $\times 10^8$ mL^{-1}. The direction of the polarizer and analyzer is indicated by white arrows.

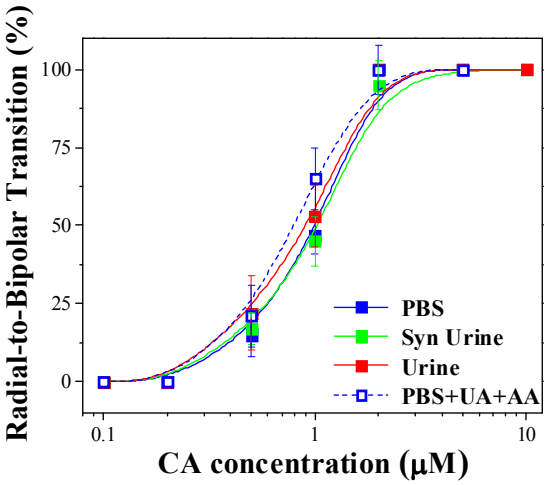

Figure 9. The bipolar-to-radial transition curves of CHI/$SC_{14}S$ complex-coated 5CB droplets as a function of CA concentrations in PBS, PBS with 250 μM UA and 250 μM AA, synthetic urine, and bovine urine.

The table of contents

Tailoring the Surface of Liquid Crystal Droplets with Chitosan/Surfactant complexes for the Selective Detection of Bile Acids in Biological Fluids

*Tanmay Bera, Jinan Deng, and Jiyu Fang**

The surface of 5CB droplets dispersed in aqueous solution is tailored by the adsorption of CHI/$SC_{14}S$ complexes at the 5CB/aqueous interface. The CHI/$SC_{14}S$ complex-coated 5CB droplets can be used as an optical probe to detect CA in biological fluids without dilution.